Scattering of Electromagnetic Waves from the Random Surface of a Left–Handed Medium

T. A. Leskova[a], A. A. Maradudin[b], and I. Simonsen[c]

[a] Institute of Spectroscopy, Rassian Academy of Sciences, Troitsk, 142090, Russia

[b] Department of Physics and Astronomy, and Institute for Surface and Interface Science
University of California, Irvine, CA 92697 U.S.A.

[c] Nordic Institute for Theoretical Physics — NORDITA
Blegdamsvej 17, DK-2100 Copenhagen Ø, Denmark

ABSTRACT

Recently a physical medium was fabricated[1] in which both the effective permittivity $\epsilon(\omega)$ and the effective permeability $\mu(\omega)$ are simultaneously negative over a restricted frequency range. Thus, in this frequency range, such a medium is "left–handed", and is characterized by a negative refractive index. A left–handed medium should exhibit unusual phenomena associated with the propagation and scattering of electromagnetic waves. In our paper we study the scattering of $p-$ and $s-$polarized electromagnetic waves from a weakly rough one–dimensional random surface of a left–handed medium. We assume that the surface profile function is a single-valued function of the coordinate in the mean plane of the surface that is normal to its grooves and ridges, and constitutes a zero-mean, stationary, Gaussian random process. We show that in contrast to nonmagnetic media with a negative dielectric function, the planar surface of a left–handed medium can support both $p-$ and $s-$polarized surface electromagnetic waves. The reflectivity of such a surface as a function of the angle of incidence displays structure associated with the existence of a Brewster angle in both polarizations and the existence of a critical angle for total internal reflection in both polarizations. The angular distribution of the intensity of the light that has been scattered incoherently displays an enhanced backscattering peak, and Yoneda bands, for both polarizations of the incident light.

Keywords: rough surface scattering, enhanced backscattering, differential reflection coefficient

1. INTRODUCTION

In a paper published in 1968, Veselago[2] showed that a medium characterized by a dielectric function $\epsilon(\omega)$ and a magnetic permeability $\mu(\omega)$ that are both negative possesses several electrodynamic properties that are different from those of a medium characterized by positive $\epsilon(\omega)$ and $\mu(\omega)$. Among them is the fact that when a plane monochromatic electromagnetic wave proportional to $\exp[i(\mathbf{k}\cdot\mathbf{x}-\omega t)]$ propagates in a medium with $\epsilon(\omega)<0$ and $\mu(\omega)<0$, the electric vector $\mathbf{E}$, the magnetic vector $\mathbf{H}$, and the wave vector $\mathbf{k}$, form a left–handed triplet of vectors. For this reason Veselago termed such a medium "left–handed". One of the consequences of the left–handedness of the medium is that the energy flux (Poynting vector) is opposite to the phase velocity of the wave. Another is that the Doppler effect is reversed, i.e. if a detector of radiation in a left–handed medium moves relative to a source that emits at a frequency ω_0 the frequency received by the detector will be smaller than ω_0, not larger as it would be in an ordinary medium ($\epsilon(\omega)>0$, $\mu(\omega)>0$). The Vavilov–Cerenkov effect is also reversed in a left–handed medium, i.e. the cone of the radiation is directed backward relative to the motion of the charged particle. Finally, in the passage of a ray from an ordinary medium across a planar boundary into a left–handed medium the refracted ray lies on the opposite side of the normal to the boundary from its position in an ordinary medium.

These electrodynamic properties of a left–handed medium remained theoretical curiosities for more than thirty years since no material could be found in nature that possessed a negative magnetic permeability. However, in recent work[3] Pendry *et al.* showed theoretically that a periodic array of nonmagnetic conducting units can be designed such that the array can be regarded as posessing an effective magnetic permeability that can become negative in a certain frequency range. In an earlier paper[4] Pendry *et al.* had shown that a structure consisting of very thin infinitely long metal wires arranged in a three–dimensional cubic structure could model the response of a dilute plasma, yielding a negative effective dielectric constant below a plasma frequency in the gigahertz range. Smith *et al.*[1] combined

Surface Scattering and Diffraction for Advanced Metrology, Zu-Han Gu, Alexei A. Maradudin, Editors,
Proceedings of SPIE Vol. 4447 (2001) © 2001 SPIE · 0277-786X/01/$15.00

these two ideas to fabricate a system consisting of a periodic array of split rings resonators, which contributed a negative effective magnetic permeability in a certain frequency range, to which parallel wires were added between the split rings, which contributed a negative effective dielectric constant in a frequency range that overlapped the range in which the effective magnetic permeability was negative, thus producing a left–handed medium. Numerical simulations and microwave transmission experiments carried out on such a system showed that it indeed behaved as a left–handed medium.

The paper by Smith *et al.*[1] stimulated a number of theoretical studies devoted to the exploration of various electrodynamic properties of left–handed media[5–10] . These include determinations[5] of the effective dielectric constant and magnetic permeability for the composite medium studied by Smith *et al.*,[1] studies of the causal properties of electromagnetic response functions of left–handed media,[6] the prediction of unusual focusing properties of a thin film of a left–handed material,[7] calculations of the scattering of an electromagnetic wave from a sphere fabricated from a left–handed medium,[8] and an investigation of surface polaritons on the planar surface of a semi–infinite left–handed medium[9] and a left-handed material slab[10] .

In this paper we study the coherent and incoherent scattering of $p-$ and $s-$polarized electromagnetic waves from the surface of a semi–infinite left–handed medium. The surface is either planar or is a one–dimensional random surface, in which case the plane of incidence is perpendicular to the generators of the surface. The interpretation of the results we obtain require a knowledge of the dispersion curves of the surface polaritons supported by the planar surface of a semi–infinite left–handed medium. We therefore study these as well, and in so doing refine some of the results obtained earlier by Ruppin.[9]

The outline of this paper, then, is as follows. In Section 2 we study some electrodynamic properties of a semi–infinite left–handed medium separated from a semi-infinite vacuum by a planar interface. Specifically, we calculate the reflectivity of the left–handed medium when it is illuminated from the vacuum side by $p-$ and $s-$polarized light, and we also obtain the dispersion relation of the surface plasmon polaritons of p and s polarization supported by this interface. The results of these calculations will be used in subsequent sections of this paper. We then turn our attention to the case where the interface between the vacuum and the left–handed medium is now a one–dimensional random interface. In Section 3 we derive the reduced Rayleigh equation for the amplitude of the scattered field when this random interface is illuminated from the vacuum side by $p-$ or $s-$polarized light whose plane of incidence is perpendicular to the generators of the interface. This equation is used as the basis of a study of the coherent (specular) scattering of $p-$ or $s-$polarized light from this interface, and the roughness–induced shifts of the Brewster angle and of the critical angle for total internal reflection are determined. It is also used in the study of the incoherent (diffuse) scattering of $p-$ or $s-$polarized light from the random surface of the left–handed medium, in particular of the enhanced backscattering peak that is now present in the angular dependence of the intensity of the scattered light of both polarizations, due to the existence of surface plasmon polaritons of both polarizations. In Section 4 numerical results and their discussion are presented. The conclusions drawn from the calculations carried out in this work are presented in Section 5.

2. The Scattering System

The system we consider in this paper consists of a vacuum in the region $x_3 > \zeta(x_1)$, and a composite medium of the kind constructed in Ref. 1 in the region $x_3 < \zeta(x_1)$. We assume that in the frequency range of interest to us the medium can be characterized by an isotropic, complex, frequency-dependent, dielectric function $\epsilon(\omega)$ and magnetic permeability $\mu(\omega)$ of the forms[5],

$$\epsilon(\omega) = 1 - \frac{\omega_p^2}{\omega(\omega + i\gamma_p)}, \tag{2.1}$$

$$\mu(\omega) = 1 - \frac{F\omega_0^2}{\omega^2 - \omega_0^2 + 2i\omega\gamma_m}, \tag{2.2}$$

where ω_p and γ_p are the effective plasma frequency and the collision frequency of the electrons of the metamaterial, and F, ω_0, and γ_m are the effective "oscillator strength", resonant frequency, and damping constant, respectively, associated with the magnetic properties of the metamaterial. We consider two different situations in the lossless case:

i) $\omega_p > \omega_m$, where $\omega_m = \omega_0\sqrt{1+F}$, $\mu(\omega_m) = 0$, i.e. the spectral range where the magnetic permeability is negative falls below the plasma frequency. Then in the frequency region $\omega_0 \leq \omega \leq \omega_m$ both $\epsilon(\omega)$ and $\mu(\omega)$ are negative and the medium is left–handed. ii) $\omega_p < \omega_m$, i.e. the medium is left–handed in the spectral range $\omega_0 \leq \omega \leq \omega_p$.

Before beginning a study of the possible effects of the "left–handedness" of the medium on the scattering of electromagnetic waves from it we first analyze the case of a planar interface between the vacuum and the medium. The Fresnel amplitude reflection coefficient for $p-$ $(r_p(k))$ and $s-$ $(r_s(k))$ polarized electromagnetic waves reflected from a medium with $\mu(\omega) \neq 1$ are given by

$$r_p(k) = \frac{\epsilon(\omega)\alpha_0(k) - \alpha(k)}{\epsilon(\omega)\alpha_0(k) + \alpha(k)}, \tag{2.3}$$

$$r_s(k) = \frac{\mu(\omega)\alpha_0(k) - \alpha(k)}{\mu(\omega)\alpha_0(k) + \alpha(k)}, \tag{2.4}$$

where $k = (\omega/c)\sin\theta_0$, θ_0 is the angle of incidence, and $\alpha_0(k) = \sqrt{(\omega^2/c^2) - k^2} = (\omega/c)\cos\theta_0$, while $\alpha(k) = \sqrt{\epsilon(\omega)\mu(\omega)(\omega^2/c^2) - k^2}$. The reflectivities of the planar surface are $R_{p,s}(\theta_0) = |r_{p,s}(k)|^2$. The function $\alpha(k)$ entering Eqs. (2.3) and (2.4), is a double–valued function of k, the corresponding branch of which must be chosen so that $Im\alpha(k) > 0$. Then, in the case where both $\epsilon(\omega)$ and $\mu(\omega)$ are negative, i.e. when the medium is left–handed, the real part of $\alpha(k)$ is negative. This reflects the fact that a left–handed medium is characterized by the negative refractive index $n(\omega) = -\sqrt{\epsilon(\omega)\mu(\omega)}$.

Several interesting properties of light reflection from and transmission through such an interface can be immediately drawn from Eqs. (2.3) and (2.4). At the frequency

$$\omega_v = \omega_p\omega_0\sqrt{\frac{1+F}{\omega_p^2 + F\omega_0^2}} \tag{2.5}$$

at which $\mu(\omega)\epsilon(\omega) = 1$ the reflectivities in both polarizations become equal and independent of the angle of incidence, $R_{p,s}(\theta_0) = |(\epsilon(\omega)+1)/(\epsilon(\omega)-1)|^2$. In the frequency region $\omega_v < \omega < \omega_m$, where the product $\epsilon(\omega)\mu(\omega)$ is smaller than unity, $\epsilon(\omega)\mu(\omega) < 1$, the phenomenon of total internal reflection occurs for both $p-$ and $s-$ polarized incident light. The critical angle for total internal reflection is then given by

$$\theta_c = \arcsin(|n(\omega)|). \tag{2.6}$$

The wavenumbers at which for the lossless interface the reflectivities vanish and become infinite, i.e. the wavenumbers of the Brewster waves and surface polaritons, respectively, are easily obtained from Eqs. (2.3) and (2.4) and are

$$k_p^2 = \frac{\omega^2}{c^2}\frac{\epsilon(\omega)(\epsilon(\omega) - \mu(\omega))}{\epsilon^2(\omega) - 1}, \tag{2.7}$$

in p polarization and

$$k_s^2 = \frac{\omega^2}{c^2}\frac{\mu(\omega)(\mu(\omega) - \epsilon(\omega))}{\mu^2(\omega) - 1} \tag{2.8}$$

in s polarization. To separate the frequency regions where surface and Brewster waves exist we define two more characteristic frequencies: ω_s, at which $\mu(\omega_s) = -1$, i.e. this is the frequency of a surface magnon ($k_s \to \infty$); and ω_ϵ, at which $\mu(\omega_\epsilon) = \epsilon(\omega_\epsilon)$ and both $k_p = 0$ and $k_s = 0$. These are given, respectively, by

$$\omega_s = \omega_0\sqrt{\frac{2+F}{2}}, \tag{2.9a}$$

$$\omega_\epsilon = \frac{\omega_p\omega_0}{\sqrt{\omega_p^2 - F\omega_0^2}}. \tag{2.9b}$$

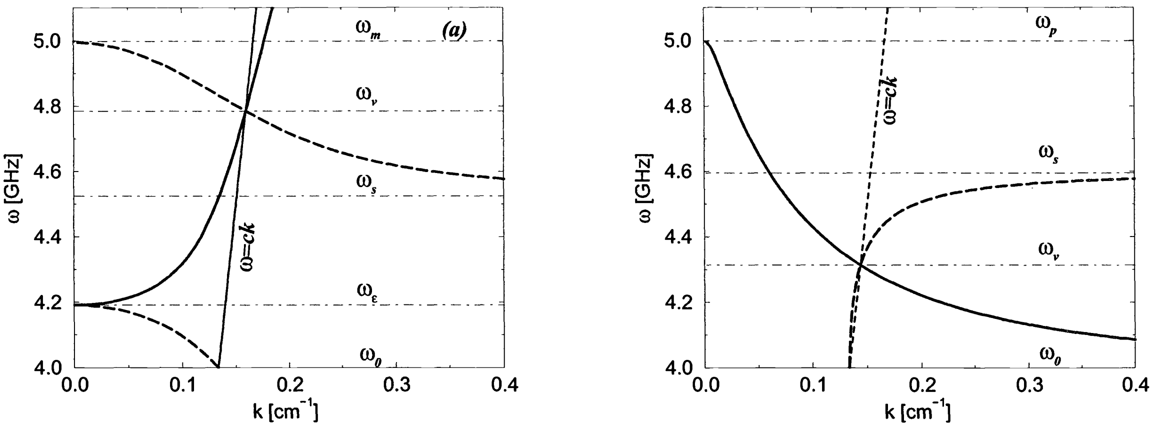

Figure 1. The dispersion curves of the surface polaritons and the Brewster waves in the case where $\omega_p > \omega_m$ (a) and $\omega_p < \omega_m$ (b).

In Figs. 1 (a) and (b) the solutions of the dispersion relations, Eqs. (2.7) and (2.8) (the frequency as a function of k_p (solid lines) and k_s (dashed lines)) are presented for two sets of material parameters: i) $\omega_p = 10$GHz, $\omega_0 = 4$GHz, $F = 0.56$ (Fig. 1 (a)); and ii) $\omega_p = 5$GHz, $\omega_0 = 4$GHz, $F = 0.64$ (Fig. 1 (b)). In the former case $\omega_m = 4.996$GHz, $\omega_s = 4.5255$GHz, $\omega_v = 4.7862$GHz, and $\omega_\epsilon = 4.1922$GHz. In the latter case $\omega_m = 5.1225$GHz, $\omega_s = 4.5957$GHz, $\omega_v = 4.3145$GHz, while ω_ϵ falls outside the frequency range where $\mu(\omega)$ and $\epsilon(\omega)$ are negative. Note that in this case the frequency of surface plasmons is $\omega_p/\sqrt{2} = 3.5255$GHz, so that in the entire frequency range where the medium is left–handed $\epsilon(\omega) > -1$, and surface polaritons do not exist in this range in ordinary metals. The vacuum light dispersion curves are shown by straight dotted lines in Figs. 1 (a) and (b). The solid curves are the dispersion curves of $p-$polarized surface polaritons and Brewster modes, while the dashed curves are the dispersion curves of $s-$polarized surface polaritons and Brewster modes. The surface polaritons exist in the nonradiative region of the $\omega - k$ plane to the right of the vacuum light line, while the Brewster modes exist in the radiative region, to the left of the vacuum light line. Thus, in the case where $\omega_p > \omega_m$ the $p-$polarized surface polaritons exist in the frequency region $\omega_v < \omega < \omega_m$, in which $\mu(\omega)\epsilon(\omega) \leq 1$. They exist also in the frequency region above ω_m ($(\omega_p/\sqrt{2}) > \omega > \omega_m$); however, there the medium becomes "normal" or "right–handed". In the frequency region $\omega_\epsilon < \omega < \omega_v$, in which $\mu(\omega)$ varies from $\epsilon(\omega)$ to $1/\epsilon(\omega)$ the $p-$polarized Brewster mode exists. The $s-$polarized surface polaritons exist in the frequency region $\omega_s < \omega < \omega_v$, i.e. in the frequency region where $\mu(\omega)$ varies from $\mu(\omega) = -1$ to $\mu(\omega) = 1/\epsilon(\omega)$. (Note that the $s-$polarized surface polaritons are due to the coupling of light with magnetic excitations, in contrast to the $p-$polarized surface polaritons that are due to the coupling of light with electric excitations.) The $s-$polarized Brewster modes exist in two frequency regions $\omega_0 < \omega < \omega_\epsilon$ $(-\infty < \mu(\omega) \leq \epsilon(\omega))$ and $\omega_v < \omega < \omega_m$ $(\epsilon^{-1}(\omega) \leq \mu(\omega) \leq 0)$. In this last frequency region the phenomenon of total internal reflection also occurs.

In the case where $\omega_p < \omega_m$ the $p-$polarized surface polaritons exist in the frequency region $\omega_0 < \omega < \omega_v$, where $\mu(\omega)$ varies from $-\infty$ to $\epsilon^{-1}(\omega)$, while the Brewster modes exist in the frequency region $\omega_v < \omega < \omega_p$, where $0 < \mu(\omega)\epsilon(\omega) < 1$ and where, therefore, total internal reflection also occurs. The $s-$polarized surface polaritons exist in the frequency region $\omega_v < \omega < \omega_s$ $(\epsilon^{-1}(\omega) < \mu(\omega) < -1)$, and the $s-$polarized Brewster modes exist in the frequency region $\omega_0 < \omega < \omega_v$ $(-\infty < \mu(\omega) < \epsilon^{-1}(\omega))$.

As mentioned in the Introduction, the dispersion of surface polaritons supported by the interface between vacuum and a left–handed medium has been studied in Ref. [9] in the case where $\omega_p > \omega_m$. We extended the analysis of electrodynamic properties of such an interface to include the radiative region of the $\omega - k$ diagram as well as the case where the material parameters of the left–handed medium are such that $\omega_m > \omega_p$. It should be noted also that the analysis of Ref. [9] is based on an expression for the magnetic permeability $\mu(\omega)$ different from Eq. (2.2).

3. The Reduced Rayleigh Equation

We assume now that the interface between the vacuum and the left–handed medium is randomly rough. The surface profile function $\zeta(x_1)$ is a single-valued function of x_1, that is differentiable as many times as is necessary, and constitutes a stationary, zero-mean Gaussian random process defined by

$$\langle\zeta(x_1)\zeta(x_1')\rangle = \delta^2 W(|x_1 - x_1'|). \tag{3.1}$$

The angle brackets in Eq. (3.1) denote an average over the ensemble of realizations of $\zeta(x_1)$, and $\delta = \langle\zeta^2(x_1)\rangle^{\frac{1}{2}}$ is the rms height of the surface.

If we introduce the Fourier representation of the surface profile function,

$$\zeta(x_1) = \int_{-\infty}^{\infty} \frac{dk}{2\pi}\hat{\zeta}(k)\exp(ikx_1), \tag{3.2}$$

the Fourier coefficient $\hat{\zeta}(k)$ is also a zero-mean Gaussian random process defined by

$$\langle\hat{\zeta}(k)\hat{\zeta}(k')\rangle = 2\pi\delta(k+k')\delta^2 g(|k|), \tag{3.3}$$

where $g(|k|)$, the power spectrum of the surface roughness, is defined by

$$g(|k|) = \int_{-\infty}^{\infty} dx_1 W(|x_1|)\exp(-ikx_1). \tag{3.4}$$

The random surface $x_3 = \zeta(x_1)$ is illuminated from the vacuum side by a $p-$ or $s-$polarized electromagnetic field of frequency ω whose plane of incidence is the x_1x_3-plane. The single nonzero component of the magnetic (p polarization) or electric (s polarization)field in the vacuum region $x_3 > \zeta(x_1)_{max}$ is then the sum of an incident wave and of scattered waves,

$$F^{>}(x_1, x_3|\omega) = \exp[ikx_1 - \alpha_0(k)x_3] + \int_{-\infty}^{\infty} \frac{dq}{2\pi} R_{p,s}(q|k)\exp[iqx_1 + i\alpha_0(q)x_3], \tag{3.5}$$

and in the medium

$$F^{<}(x_1, x_3|\omega) = \int_{-\infty}^{\infty} \frac{dq}{2\pi} T(q|k)\exp[iqx_1 - i\alpha(q)x_3], \tag{3.6}$$

where

$$\alpha_0(q) = [(\omega/c)^2 - q^2]^{\frac{1}{2}} \qquad Im\alpha_0(q) > 0, Re\alpha_0(q) > 0, \tag{3.7}$$

and

$$\alpha(q) = [\epsilon(\omega)\mu(\omega)(\omega/c)^2 - q^2]^{\frac{1}{2}} \qquad Im\alpha(q) > 0, Re\alpha(q) < 0. \tag{3.8}$$

Matching the tangential components of the magnetic and electric fields across the surface and eliminating from the equations thus obtained the amplitude of the transmitted field $T(q|k)$, we obtain the reduced Rayleigh equation for the scattering amplitude $R(q|k)$ in the standard form:

$$\int_{-\infty}^{\infty} \frac{dq}{2\pi} N_{p,s}^{(+)}(p|q)R_{p,s}(q|k) = -N_{p,s}^{(-)}(q|k), \tag{3.9}$$

where

$$N_p^{(\pm)}(p|q) = \left[\left(1 - \frac{1}{\epsilon(\omega)}\right)(pq \pm \alpha(p)\alpha_0(q))(\mu(\omega) - 1)\frac{\omega^2}{c^2}\right]\frac{I(\alpha(p) \mp \alpha_0(q)|p-q)}{\alpha(p) \mp \alpha_0(q)}, \tag{3.10a}$$

$$N_s^{(\pm)}(p|q) = \left[\left(1 - \frac{1}{\mu(\omega)}\right)(pq \pm \alpha(p)\alpha_0(q)) + (\epsilon(\omega) - 1)\frac{\omega^2}{c^2}\right]\frac{I(\alpha(p) \mp \alpha_0(q)|p-q)}{\alpha(p) \mp \alpha_0(q)}, \tag{3.10b}$$

and

$$I(\gamma|Q) = \int_{-\infty}^{\infty} dx_1 e^{-iQx_1}e^{-i\gamma\zeta(x_1)}. \tag{3.11}$$

The contribution to the mean differential reflection coefficient (drc) from the light scattered incoherently is given in terms of the scattering amplitude $R(q|k)$ by

$$\left\langle\frac{\partial R_{p,s}}{\partial\theta_s}\right\rangle_{incoh} = \frac{1}{L_1}\frac{\omega}{2\pi c}\frac{\cos^2\theta_s}{\cos\theta_0}[\langle|R_{p,s}(q|k)|^2\rangle - |\langle R_{p,s}(q|k)\rangle|^2], \tag{3.12}$$

where L_1 is the length of the x_1-axis covered by the random surface, and θ_0 and θ_s are the angles of incidence and scattering, respectively, measured counterclockwise and clockwise from the x_3-axis, and are related to the wavenumbers k and q by

$$k = (\omega/c)\sin\theta_0, \qquad q = (\omega/c)\sin\theta_s. \tag{3.13}$$

The contribution to the mean drc from the coherent component of the scattered light is given by

$$\left\langle\frac{\partial R_{p,s}}{\partial\theta_s}\right\rangle_{coh} = \frac{1}{L_1}\frac{\omega}{2\pi c}\frac{\cos^2\theta_s}{\cos\theta_0}|\langle R_{p,s}(q|k)\rangle|^2. \tag{3.14}$$

In the case where the surface is weakly rough we use the self–energy perturbation approach[11] to calculate the reflectivity, and small–amplitude perturbation theory[12] to calculate the contribution to the mean differential reflection coefficient from the incoherent component of the scattered light. In the case of a moderately rough surface we solve Eq. (3.9) numerically.

In the self–energy perturbation theory the ensemble average of $R(q|k)$ that we need in order to calculate the reflectivity is given by[11]

$$\langle R_{p,s}(q|k)\rangle = -2\pi\delta(q-k) - 2i\langle G_{p,s}(q|k)\rangle\alpha_0(k), \tag{3.15}$$

where $G_{p,s}(q|k)$ is the Green's function associated with the randomly rough interface between the vacuum and the scattering medium. Due to the stationarity of $\zeta(x_1)$ the averaged Green's function $\langle G(q|k)\rangle$ appearing in Eq. (3.15) has the form[11]

$$\langle G_{p,s}(q|k)\rangle = 2\pi\delta(q-k)G_{p,s}(k) = 2\pi\delta(q-k)\frac{1}{[G_{p,s}^{(0)}(k)]^{-1} - M_{p,s}(k)}, \tag{3.16}$$

where $G_{p,s}(k)$ is the averaged Green's function and $M_{p,s}(k)$ is the averaged proper self–energy. The latter is given by

$$\langle M_{p,s}(q|k)\rangle = 2\pi\delta(q-k)M_{p,s}(k), \tag{3.17}$$

where the (unaveraged) proper self–energy $M_{p,s}(q|k)$ is the solution of[11]

$$M_{p,s}(q|k) = V_{p,s}(q|k) + \int_{-\infty}^{\infty}\frac{dp}{2\pi}\int_{-\infty}^{\infty}\frac{dr}{2\pi}M_{p,s}(q|p)\langle G_{p,s}(p|r)\rangle[V_{p,s}(r|k) - \langle M_{p,s}(r|k)\rangle], \tag{3.18}$$

where the scattering potential $V_{p,s}(p|k)$ satisfies the integral equation

$$\int_{-\infty}^{\infty} \frac{dq}{2\pi} \left[N_{p,s}^{(-)}(p|q) - N_{p,s}^{(+)}(p|q)\right] \frac{V_{p,s}(q|k)}{2\alpha_0(q)} = \frac{N_{p,s}^{(-)}(p|k) + N_{p,s}^{(+)}(p|k)(1 + 2i\alpha_0(k)G_{p,s}^{(0)}(k))}{2\alpha_0(k)G_{p,s}^{(0)}(k))}. \tag{3.19}$$

In Eq. (3.19)

$$G_p^{(0)}(q) = \frac{i\epsilon(\omega)}{\epsilon(\omega)\alpha_0(q) + \alpha(q)} \tag{3.20}$$

in the case of p polarization, and

$$G_s^{(0)}(q) = \frac{i\mu(\omega)}{\mu(\omega)\alpha_0(q) + \alpha(q)} \tag{3.21}$$

in the case of s polarization, are the Green's functions associated with a planar surface. When the explicit expressions for $G_{p,s}^{(0)}(k)$ are used in Eq. (3.16), we find that

$$\langle R_{p,s}(q|k)\rangle = 2\pi\delta(q-k)r_{p,s}(\theta_0), \tag{3.22}$$

where

$$r_p(\theta_0) = \frac{\epsilon(\omega)\alpha_0(k) - \alpha(k) + i\epsilon(\omega)M_p(k)}{\epsilon(\omega)\alpha_0(k) + \alpha(k) - i\epsilon(\omega)M_p(k)}, \tag{3.23a}$$

$$r_s(\theta_0) = \frac{\mu(\omega)\alpha_0(k) - \alpha(k) + i\mu(\omega)M_s(k)}{\mu(\omega)\alpha_0(k) + \alpha(k) - i\mu(\omega)M_s(k)}. \tag{3.23b}$$

4. Results

We first present numerical results for the reflectivities $R_p(\theta_0)$ and $R_s(\theta_0)$. In obtaining these results we have assumed that the surface roughness is characterized by a Gaussian power spectrum with the rms height $\delta = 0.4$cm and the transverse correlation length $a = 4$cm. The damping constants entering the expressions for $\epsilon(\omega)$ and $\mu(\omega)$ are $\gamma_p = 0.001\omega_p$ and $\gamma_m = 0$. In Fig. 2 (a) we plot the logarithm of $R_p(\theta_0)$ and $R_s(\theta_0)$ calculated for the case where $\omega_p > \omega_m$, which was illustrated in Fig. 1 (a). The solid lines are the reflectivities of the rough surface and the dashed lines are the reflectivities of the planar surface. The frequency of the incident light, $\omega = 4.4$GHz in the case of $p-$polarized light and $\omega = 4.1$GHz in the case of $s-$polarized light, lies in the range of existence of the Brewster angle. In Fig. 2 (b) $R_p(\theta_0)$ and $R_s(\theta_0)$ are plotted for the case where the incident light frequency $\omega = 4.8$GHz is in the interval where total internal reflection occurs. Note that the reflectivity of $s-$polarized light in Fig. 2 (b) displays both the Brewster angle and total internal reflection. Although the surface roughness is quite weak, the shift of the Brewster angles in both p and s polarizations is clearly seen in Fig. 2 (a). At the higher frequency, $\omega = 4.8$GHz (Fig. 2 (b)), the effect of roughness is strong for $p-$polarized light and is very weak for $s-$polarized light. The reflectivities for $p-$ and $s-$polarized light for the case where $\omega_p < \omega_m$, which was illustrated in Fig. 1(b), are shown in Fig. 3. As seen from Figs. 2 and 3 the influence of roughness on the reflectivities is much weaker in the case where $\omega_p < \omega_m$ than in the case where $\omega_p > \omega_m$. In the frequency region of total internal reflection (see, Figs. 2 (b) and 3 (b)) the effect of the surface roughness is strong for $p-$polarized light and is weak for $s-$polarized light in the case where $\omega_p > \omega_m$ (Fig. 2 (b)), while it is stronger in s polarization than in p polarization in the case where $\omega_p < \omega_m$ (Fig. 3 (b)).

The contributions to the mean differential reflection coefficient from the light scattered incoherently from the randomly rough interface between the vacuum and the left–handed medium for different frequencies of the incident light in the case where $\omega_p > \omega_m$ are shown in Fig. 4, and in the case where $\omega_p < \omega_m$ in Fig. 5. The roughness parameters are $\delta = 0.2$cm and $a = 4$cm. The angle of incidence is $\theta_0 = 0°$. The curves in Fig. 4 (a) and (b) show the evolution of the angular distribution of the intensity of the scattered light with the frequency of the incident light. The lowest curve in Fig. 4 (a) is the drc calculated for the frequency $\omega = 4.75$GHz of the incident light, which falls

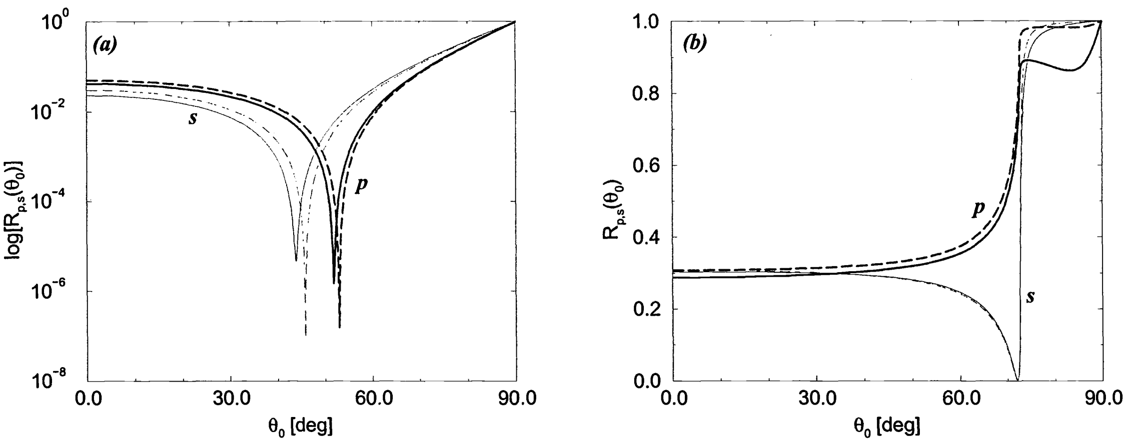

Figure 2. The reflectivities $R_p(\theta_0)$ (thick lines) and $R_s(\theta_0)$ (thin lines) calculated for the case where $\omega_p > \omega_m$. (a) $\omega = 4.2$GHz (p polarization) and $\omega = 4.1$GHz (s polarization); (b) $\omega = 4.8$GHz. The dashed curves are the reflectivities of the corresponding planar surface.

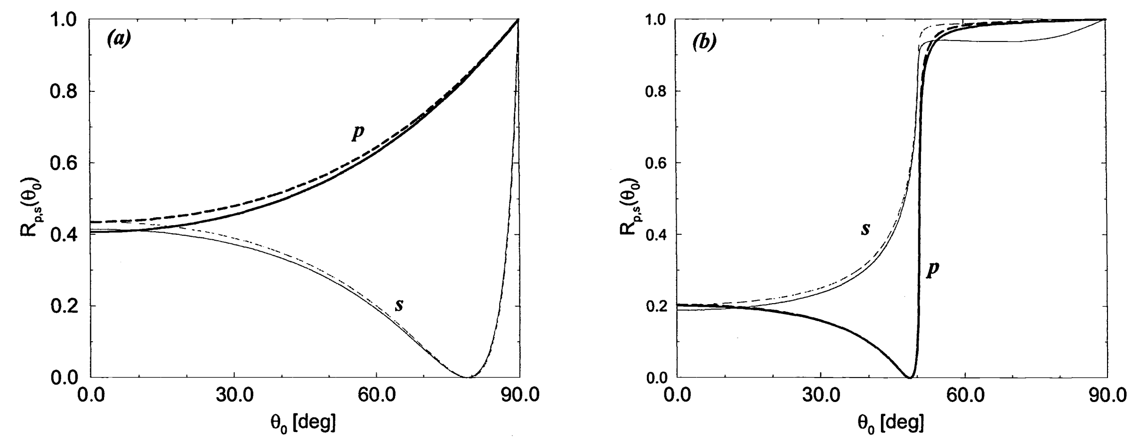

Figure 3. The reflectivities $R_p(\theta_0)$ (thick lines) and $R_s(\theta_0)$ (thin lines) calculated for the case where $\omega_p < \omega_m$. (a) $\omega = 4.1.$GHz and (b) $\omega = 4.4$GHz. The dashed curves are the reflectivities of the corresponding planar surface.

into the range where the scattering medium does not support surface polaritons. When the frequency of the incident light increases and falls into the frequency region above ω_v ($\omega = 4.8$GHz, $\omega = 4.9$GHz, and $\omega = 4.98$GHz in our case), the multiple scattering of surface polaritons leads to the appearance of an enhanced backscattering peak. The strong wings in Fig. 4 (a) are the Yoneda bands[13], which are due to the total internal reflection of the scattered light. The plots in Fig. 4 (b) were calculated for the frequencies of the incident $s-$polarized light which fall into different characteristic frequency ranges. When the frequency of the incident light is below ω_s ($\omega = 4.5$GHz in our case), where surface polaritons of s polarization do not exist, the drc is structureless. When the frequency of the incident light falls in the region of surface polariton existence ($\omega = 4.6$GHz in our example), the incoherent scattering is increased strongly and an enhanced backscattering peak is displayed. The plot for the frequency $\omega = 4.8$GHz displays well pronounced Yoneda bands and no enhanced backscattering peak since this frequency lies in the region where the

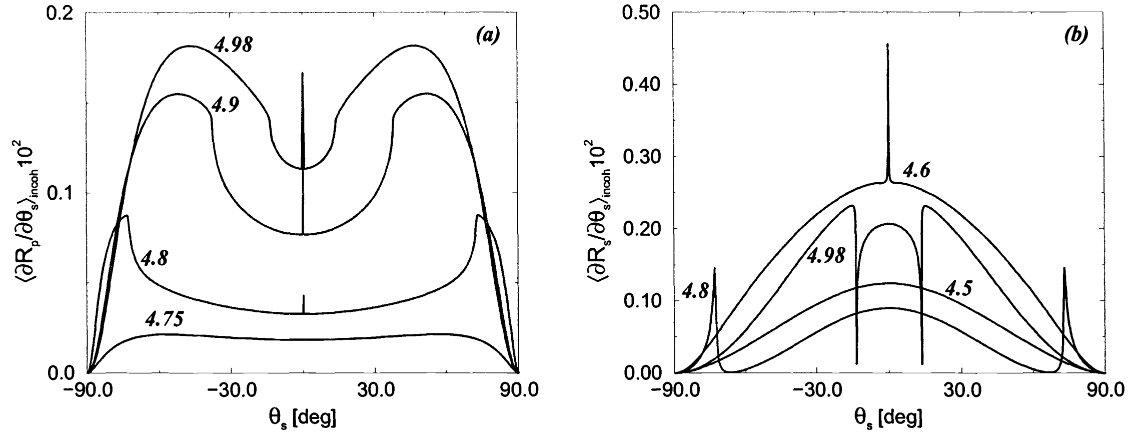

Figure 4. (a) The contribution to the mean differential reflection coefficient from the diffusely scattered $p-$polarized light. The frequencies of the incident light (in GHz) are shown in the Figure. (b) the same as in (a) but for $s-$polarized light.

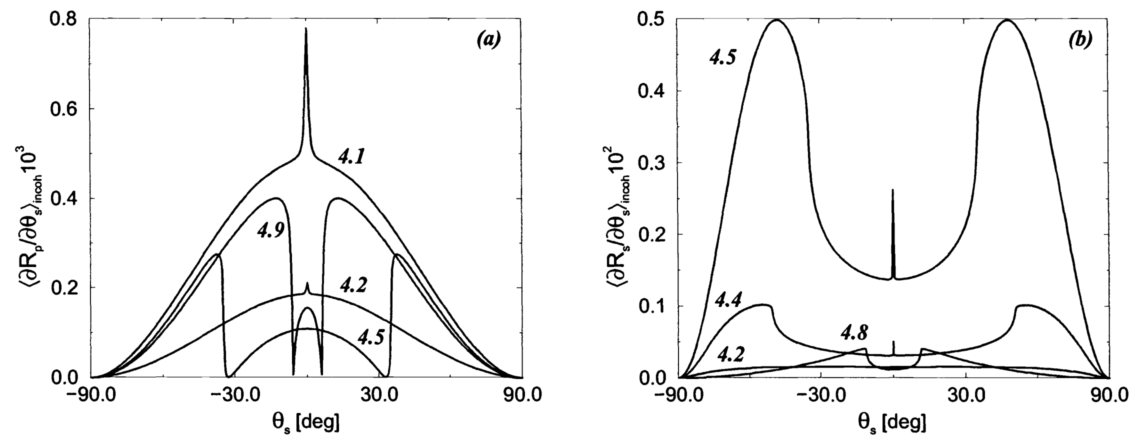

Figure 5. (a) The contribution to the mean differential reflection coefficient from the $p-$polarized light scattered incoherently. The frequencies of the incident light (in GHz) are shown in the Figure. (b) the same as in (a) but for $s-$polarized light.

surface of the left–handed medium does not support surface polaritons but total internal reflection of the scattered light occurs. With the further increase of the frequency ($\omega = 4.98$GHz) the Yoneda bands evolve into narrow dips in the plot for $\omega = 4.98$GHz, which are due to the sharp drop (the quasi–Brewster effect) of the reflectivity in the immediate vicinity of the critical angle for total internal reflection.

As expected, in the case where $\omega_p < \omega_m$ the contribution to the mean differential reflection coefficient from the diffusely scattered $p-$polarized light (Fig. 5 (a)) displays an enhanced backscattering peak if the frequency of the incident light is smaller than ω_v ($\omega_0 < \omega < \omega_v$), while in the frequency region $\omega > \omega_v$ it display the Yoneda bands and the quasi–Brewster effect. The situation is different for $s-$polarized incident light (Fig. 5 (b)). In this case the contribution to the mean differential reflection coefficient from the diffusely scattered light is structureless for

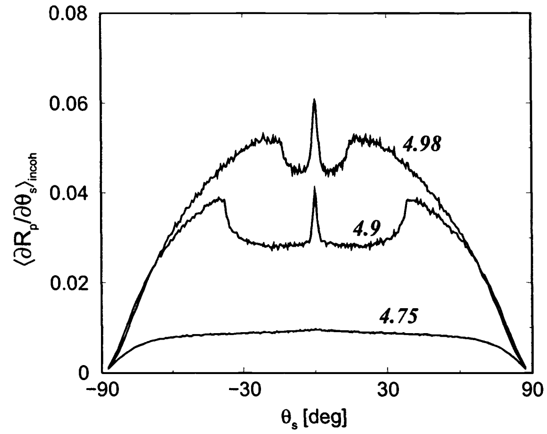

Figure 6. The contribution to the mean differential reflection coefficient from the p−polarized light scattered incoherently from a strongly rough surface of the left–handed medium. The frequencies of the incident light (in GHz) are shown in the Figure.

frequencies below ω_v, and displays an enhanced backscattering peak and Yoneda bands when the frequency of the incident light is in the interval between ω_v and ω_m, where the s−polarized surface polaritons exist and total internal reflection occurs. As the frequency increases and passes into the interval $\omega_v < \omega < \omega_p$ $\langle \partial R_s / \partial \theta_s \rangle_{incoh}$ displays the Yoneda bands. It should be pointed out here that due to the nonzero magnetic susceptibility of the medium the single–scattering processes are strongly suppressed. Finally, in Fig. 6 the contribution to the mean differential reflection coefficient from the p−polarized light scattered incoherently from a strongly rough surface of the left–handed medium is plotted. These results were obtained by a direct numerical solution of the reduced Rayleigh equation Eq. (3.9) [14]. The material parameters are the same as those used in obtaining Figs. 1 (a), 2, and 4. The roughness parameters are $\delta = 1$cm and $a = 8$cm. The plots should be compared with those shown in Fig. 4 (a).

5. Conclusions

In this paper we have calculated the dispersion curves of surface polaritons of both p and s polarization that occur at the planar interface between vacuum and a left–handed medium. In so doing we have refined some of the results for these dispersion curves obtained recently by Ruppin[9]. In addition, we have shown that the left–handedness of the scattering medium leads to curious frequency and angular dependences of the reflectivity of such a medium bounded by a one–dimensional randomly rough surface, and of the angular dependence of the intensity of the light scattered incoherently from such a surface. Thus, the reflectivities of both p− and s−polarized light display the Brewster effect and the phenomenon of total internal reflection in suitable ranges of the frequency of the incident light. The roughness induced shifts of the Brewster angle and of the critical angle for total internal reflection have also been calculated. In addition, both perturbative and nonperturbative solutions of the reduced Rayleigh equation have shown that an enhanced backscattering peak is present in the angular dependence of the intensity of the incoherently scattered light of both polarizations, as well as Yoneda bands.

ACKNOWLEDGEMENTS

This research was supported in part by Army Research Grant No. DAAG 55–98–C–0034.

REFERENCES

1. D.R.Smith, W.J. Padilla, D.C. Vier, S.C. Nemat-Nasser, and S. Schultz, "Composite media with simultaneously negative permeability and permittivity," Phys. Rev. Lett. **84**, 4184-4187 (2000).

2. V.G. Veselago, "The electrodynamics of substances with simultaneously negative values of ϵ and μ," Sov.Phys.Uspekhi **10**, 509-514 (1968).
3. J.B. Pendry, A.J. Holden, D.J.Robbins, and W.J. Stewart, "Magnetism from conductors and enhanced nonlinear phenomena," IEEE Trans. Microwave Theory Tech. **47**, 2075-2084 (1999).
4. J.B. Pendry, A.J. Holden, W.J. Stewart, and I.Youngs, "Extremly low frequency plasmons in metallic mesostructures," Phys.Rev.Lett. **76**, 4773-4780 (1996).
5. D. R. Smith, D.C. Vier, N. Kroll, and S. Schultz, " Direct calculation of permeability and permittivity for a left–handed metamaterial," Appl. Phys. Lett. **77**, 2246-2248 (2000).
6. D. R. Smith and N. Kroll, "Negative refractive index in left–handed materials," Phys. Rev. Lett. **85**, 2933-2936 (2000).
7. J.B. Pendry, "Negative refraction index makes a perfect lens," Phys. Rev. Lett. **85**, 3966-3969 (2000).
8. R. Ruppin, "Extinction properties of a sphere with negative permittivity and permeability," Solid State Commun. **116**, 411-415 (2000).
9. R. Ruppin, "Surface polaritons of a left–handed medium," Phys. Lett. A**277**, 61-64 (2000).
10. R. Ruppin, "Surface polaritons of a left-handed material slab," J.Phys.: Condensed Matter **13**, 1811-1818 (2001).
11. G.C. Brown, V. Celli, M. Haller, A.A. Maradudin, and A. Marvin, "Resonant light scattering from a randomly rough surface," Phys. Rev. B **31**, 4993-5005 (1985).
12. S.O. Rice, "Reflection of electromagnetic waves from slightly rough surfaces," Commun. Pure Appl. Math. **4**, 351-378 (1951).
13. Y. Yoneda, "Anomalous surface reflection of X rays," Phys. Rev. **131**, 2010-2013 (1963).
14. I. Simonsen, and A. A. Maradudin, "Numerical simulation of electromagnetic wave scattering from planar dielectric films deposited on rough perfectly conducting substrates," Opt. Commun. **162**, 99-111 (1999).